AAS 01-110

SIMULTANEOUS PRECESSION MANEUVER AND ACTIVE NUTATION CONTROL

Sergei Tanygin*

Simultaneous precession maneuver and active nutation control is proposed for axisymmetric spinners. Nominally, only certain ratios of inertia moments facilitate nutation cancellation during precession maneuver. Spacecraft with other ratios may be subjected to significant residual nutation, which may need to be actively controlled. The proposed method modifies start and stop times of each pulse during the precession maneuver in order to reduce residual nutation while maintaining precession accuracy. Parametric studies indicate significant potential fuel and time savings as well as overall accuracy improvements.

INTRODUCTION

Spin-stabilized spacecraft can be very simple and fuel efficient, which makes this option particularly attractive for small spacecraft. A number of larger spacecraft are also spinning at least during some phase of their lifetime[1-4]. During spinning, the spacecraft reorientation is accomplished using precession maneuver. This involves pulsing the offset axial thruster at times when the applied torque can move the angular momentum vector in the desired direction. This induces nutation of the axisymmetric spacecraft, which moves its spin axis. With the appropriate choice of inertia moments, the nutation can be cancelled later and spacecraft placed into a pure spin about its new inertial orientation.[2,4] If inertia moments do not have certain ratios, the nutation will not be fully cancelled and can actually grow quite large. Rigid oblate spinners and prolate spinners may require active nutation control (ANC) to cancel residual nutation.[4] The method proposed in this paper modifies precession maneuver in such a way so as reduce residual nutation for a wide range inertia moments while maintaining precession accuracy. If this is accomplished, it can lead to better pointing accuracy as well as fuel and time savings.

EQUATIONS OF MOTION

The first step in developing of the proposed method consists of formulating equations of motion, initially, for a single pulse and, then, for multiple pulses. The equations

* Member AAS and AIAA. Sr. Astro-Development Specialist, Analytical Graphics, Inc., 325 Technology Dr., Malvern, PA 19355, stanygin@stk.com

are derived under the assumptions that the spacecraft is an axisymmetric rigid body and that pulses are represented by the ideal square wave. The effect caused by violations of these assumptions is discussed in subsequent sections. The following notation is used throughout this paper. The oblateness parameter indicates degree of asymmetry of the spacecraft:

$$\sigma \equiv I_a / I_t , \tag{1}$$

where I_a and I_t are the axial and the transverse moments of inertia, respectively. The parameter is greater than 1 for an oblate spacecraft (e.g. disc shaped) and is less than 1 for a prolate spacecraft (e.g. rod shaped). Values farther away from 1 in either direction indicate a more asymmetric spacecraft. Oblateness of 1 corresponds to a symmetric spacecraft (e.g. sphere). The body observed nutation frequency indicates how fast the angular velocity vector is seen rotating about the angular momentum vector:

$$\lambda \equiv (\sigma - 1)\Omega , \tag{2}$$

where Ω is the spin rate about spacecraft's axis of symmetry (or spin axis). That same motion observed in the inertial frame has frequency $\lambda + \Omega = \sigma\Omega$. A thruster located on the side of the spacecraft and firing along the spin axis passes through its desired precession alignment every integer number of spin periods. Any multiplicity of spin periods can be used as the pulse cycle period:

$$T \equiv 2\pi k / \Omega , \; k = 1,2,3,... , \tag{3}$$

but the fastest and simplest strategy calls for pulsing during every revolution of the spacecraft, i.e. $k = 1$. All pulses are assumed to have the same duration Δt, which does not need to be small in derivations below. However, given that the same thrust impulse

$$I_F \equiv F\Delta t , \tag{4}$$

where F is the magnitude of the resultant force, is more effective if produced during shorter pulses, a useful simplification can be obtained for $|\Omega\Delta t| << 1$. The derivations in this section seek to decouple the motion of the spin axis from the spin itself. In doing so, a shorthand notation for two-dimensional parameterization of the former is convenient. The two-dimensional vector of transverse angular velocity components is denoted as $\boldsymbol{\omega} \equiv [\omega_1 \quad \omega_2]^{\mathrm{T}}$. Another two-dimensional vector contains angles, which define the spin axis direction. The vector is introduced as $\boldsymbol{\theta} \equiv [\theta_1 \quad \theta_2]^{\mathrm{T}}$, where the angles are collected from the $\theta_2 - \theta_1 - \theta_3$ Euler sequence. Finally, two-dimensional (planar) counterclockwise rotation is mechanized via the following operator

$$\mathbf{R}\{\alpha\} \equiv \begin{bmatrix} \cos\alpha & -\sin\alpha \\ \sin\alpha & \cos\alpha \end{bmatrix}, \tag{5}$$

where α is the angle of rotation.

Another parameter is introduced:

$$\boldsymbol{\omega}_{\mathbf{p}} \equiv \frac{\sigma}{(\sigma-1)h_a}\mathbf{R}\left\{\frac{\pi}{2}\right\}\mathbf{M}, \tag{6}$$

which represents the influence of two-dimensional vector of transverse torque components, $\mathbf{M} \equiv \begin{bmatrix} M_1 & M_2 \end{bmatrix}^{\mathrm{T}}$, on the transverse angular acceleration $\dot{\boldsymbol{\omega}}$, where $h_a \equiv I_a\Omega$ is the axial angular momentum.

The attitude motion during any given pulse cycle is broken into three phases. The first phase precedes the pulse and the last phase succeeds it. The ith pulse cycle starts at time t_{i-1} with its pre-pulse phase nominally running until $t_{i-1,*} \equiv t_{i-1} + t_* - \Delta t/2$ and post-pulse phase nominally starting at $t_{*,i} \equiv t_{i-1,*} + \Delta t$. The next pulse starts at $t_i \equiv t_{i-1} + T$. The nominal mid-time of the pulse, t_*, is the same within each pulse cycle. Without loss of generality, the pulse can be positioned in the middle of each cycle, $t_* \equiv T/2$, thus, introducing convenient symmetry into the problem. This is possible because the start time of the first pulse can be always adjusted so that the pulses initiate desired precession. The fundamental idea of the proposed method consists of adding small time adjustments, δt_i, to each pulse, such that the adjustment simultaneously moves ith pulse start time, $t_{i-1,\delta} \equiv t_{i-1,*} + \delta t_i$, and its stop time, $t_{\delta,i} \equiv t_{*,i} + \delta t_i$, thus, preserving the pulse duration, Δt.

During each phase, the angular velocity can be integrated in closed-form. The transverse torque only affects the transverse angular velocity components, which are found as follows:[5,6]

$$\boldsymbol{\omega}(t) = \mathbf{R}\{\lambda(t - t_{i-1})\}\boldsymbol{\omega}_{\mathbf{i-1}},\ t_{i-1} \le t \le t_{i-1,\delta},\ \boldsymbol{\omega}_{\mathbf{i-1,\delta}} \equiv \boldsymbol{\omega}(t_{i-1,\delta}), \tag{7}$$

$$\boldsymbol{\omega}(t) = \mathbf{R}\{\lambda(t - t_{i-1,\delta})\}(\boldsymbol{\omega}_{\mathbf{i-1,\delta}} - \boldsymbol{\omega}_{\mathbf{p}}) + \boldsymbol{\omega}_{\mathbf{p}},\ t_{i-1,\delta} < t \le t_{\delta,i},\ \boldsymbol{\omega}_{\boldsymbol{\delta,\mathrm{i}}} \equiv \boldsymbol{\omega}(t_{\delta,i}), \tag{8}$$

$$\boldsymbol{\omega}(t) = \mathbf{R}\{\lambda(t - t_{\delta,i})\}\boldsymbol{\omega}_{\boldsymbol{\delta,\mathrm{i}}},\ t_{\delta,i} < t \le t_i,\ \boldsymbol{\omega}_{\mathrm{i}} \equiv \boldsymbol{\omega}(t_i). \tag{9}$$

Their evolution spanning all three phases is a piecewise smooth function of time, which will be further used to solve for attitude kinematics.

Ability to approximate attitude motion in closed-form depends greatly on the choice of attitude parameterization. Judicious selection of non-symmetrical Euler angle sequence "precession-deviation-spin" facilitates development of the closed-form attitude solution during the precession maneuver. Without loss of generality, let the precession be defined about the reference inertial i_2 axis and the deviation be defined about the precessing (but not spinning) a_1 axis. This way the deviation can be interpreted as the angle between the spin axis and the precession plane. Finally, the spin angle is defined about the body e_3 axis, which is consistent with the selection of the axial angular velocity component. This sequence of

Euler angles is not only convenient geometrically, but also permits linearization of the attitude kinematics using only one small angle assumption.[1,4] Namely, the deviation is assumed small, which is reasonable as the proposed method seeks to minimize it. Thus, the linearized attitude kinematics become

$$\dot{\boldsymbol{\theta}}(t) \approx \mathbf{R}\{\Omega t\}\boldsymbol{\omega}(t)\,,\ \theta_1 << 1\,. \tag{10}$$

The resulting approximate Euler angle derivatives are piecewise integrable in closed-form.

$$\boldsymbol{\theta}_\mathbf{i} \equiv \boldsymbol{\theta}(t_i)\ ,\ \boldsymbol{\theta}_{\mathbf{i-1}} \equiv \boldsymbol{\theta}(t_{i-1})$$

$$\boldsymbol{\theta}_\mathbf{i} = \boldsymbol{\theta}_{\mathbf{i-1}} + \int_{t_{i-1}}^{t_{i-1,\delta}} \mathbf{R}\{\Omega t\}\boldsymbol{\omega}(t)dt + \int_{t_{i-1,\delta}}^{t_{\delta,i}} \mathbf{R}\{\Omega t\}\boldsymbol{\omega}(t)dt + \int_{t_{\delta,i}}^{t_i} \mathbf{R}\{\Omega t\}\boldsymbol{\omega}(t)dt \tag{11}$$

This formula along with the formula for the transverse angular velocity (Eqs.6-8) can be rewritten as functions of the adjustment, δt_i,

$$\boldsymbol{\omega}_\mathbf{i} = \mathbf{A}_\boldsymbol{\omega}(\delta t_i)\boldsymbol{\omega}_{\mathbf{i-1}} + \mathbf{B}_\boldsymbol{\omega}(\delta t_i)\boldsymbol{\omega}_\mathbf{p}\,, \tag{12}$$

$$\boldsymbol{\theta}_\mathbf{i} = \boldsymbol{\theta}_{\mathbf{i-1}} + \mathbf{A}_\boldsymbol{\theta}(\delta t_i)\boldsymbol{\omega}_{\mathbf{i-1}} + \mathbf{B}_\boldsymbol{\theta}(\delta t_i)\boldsymbol{\omega}_\mathbf{p} \tag{13}$$

and then further modified to isolate terms linear in δt_i:

$$\boldsymbol{\omega}_\mathbf{i} = \mathbf{A}_{\boldsymbol{\omega}\mathbf{0}}\boldsymbol{\omega}_{\mathbf{i-1}} + \left(\mathbf{B}_{\boldsymbol{\omega}\mathbf{0}} + \mathbf{B}_{\boldsymbol{\omega}\mathbf{t}}\delta t_i\right)\boldsymbol{\omega}_\mathbf{p} + o(\delta t_i^2)\,, \tag{14}$$

$$\boldsymbol{\theta}_\mathbf{i} = \boldsymbol{\theta}_{\mathbf{i-1}} + \mathbf{A}_{\boldsymbol{\theta}\mathbf{0}}\boldsymbol{\omega}_{\mathbf{i-1}} + \left(\mathbf{B}_{\boldsymbol{\theta}\mathbf{0}} + \mathbf{B}_{\boldsymbol{\theta}\mathbf{t}}\delta t_i\right)\boldsymbol{\omega}_\mathbf{p} + o(\delta t_i^2)\,. \tag{15}$$

The resulting expressions can be interpreted as a single pulse cycle state transition equation

$$\mathbf{x}_\mathbf{i} = \mathbf{A}_\mathbf{0}\mathbf{x}_{\mathbf{i-1}} + \left(\mathbf{B}_\mathbf{0} + \mathbf{B}_\mathbf{t}\delta t_i\right)\boldsymbol{\omega}_\mathbf{p} + o(\delta t_i^2)\,, \tag{16}$$

where the state is defined as $\mathbf{x}_\mathbf{i} \equiv \begin{bmatrix}\boldsymbol{\theta}_\mathbf{i}\\ \boldsymbol{\omega}_\mathbf{i}\end{bmatrix}$, the matrices are constructed as $\mathbf{A}_\mathbf{0} \equiv \begin{bmatrix}\mathbf{E} & \mathbf{A}_{\boldsymbol{\theta}\mathbf{0}}\\ \mathbf{0} & \mathbf{A}_{\boldsymbol{\omega}\mathbf{0}}\end{bmatrix}$, $\mathbf{B}_\mathbf{0} \equiv \begin{bmatrix}\mathbf{B}_{\boldsymbol{\theta}\mathbf{0}}\\ \mathbf{B}_{\boldsymbol{\omega}\mathbf{0}}\end{bmatrix}$, $\mathbf{B}_\mathbf{t} \equiv \begin{bmatrix}\mathbf{B}_{\boldsymbol{\theta}\mathbf{t}}\\ \mathbf{B}_{\boldsymbol{\omega}\mathbf{t}}\end{bmatrix}$ and their exact form is shown in the appendix. Finally, straightforward repeated application of the single pulse cycle transition results in the following N pulse cycle transition equation:

$$\mathbf{x}_\mathbf{N} = \mathbf{A}_\mathbf{0}^\mathbf{N}\mathbf{x}_\mathbf{0} + \sum_{j=0}^{N-1}\mathbf{A}_\mathbf{0}^\mathbf{j}\mathbf{B}_\mathbf{0}\boldsymbol{\omega}_\mathbf{p} + \sum_{j=0}^{N-1}\mathbf{A}_\mathbf{0}^\mathbf{j}\mathbf{B}_\mathbf{t}\boldsymbol{\omega}_\mathbf{p}\delta t_{N-j} + o(\delta t_k \delta t_l)\,,\ k,l = 1,2,...,N\,, \tag{17}$$

where $\mathbf{x}_\mathbf{0}$ is the initial state.

MINIMUM-NORM SOLUTION

Transition equation developed in the previous section relates the initial state with the state after N pulse cycles. This relationship can be explored to determine how to reach the desired target state using N pulse time adjustments. A reasonable way to define this target state is by first computing the state after N nominal pulses:

$$\bar{\mathbf{x}}_{\mathbf{N}} = \mathbf{A}_{\mathbf{0}}^{\mathbf{N}}\mathbf{x}_{\mathbf{0}} + \sum_{j=0}^{N-1}\mathbf{A}_{\mathbf{0}}^{\mathbf{j}}\mathbf{B}_{\mathbf{0}}\boldsymbol{\omega}_{\mathbf{p}}\,. \tag{18}$$

Then this state is converted into the desired target state, $\hat{\mathbf{x}}_{\mathbf{N}}$, by zeroing its transverse angular velocity and deviation components:

$$\bar{\mathbf{x}}_{\mathbf{N}} = \begin{bmatrix}\bar{\theta}_1 & \bar{\theta}_2 & \bar{\omega}_1 & \bar{\omega}_2\end{bmatrix}^{\mathbf{T}} \Rightarrow \hat{\mathbf{x}}_{\mathbf{N}} = \begin{bmatrix}0 & \bar{\theta}_2 & 0 & 0\end{bmatrix}^{\mathbf{T}}. \tag{19}$$

The target vector is defined as the difference between the target state and the nominal state:

$$\mathbf{y}_{\mathbf{N}} \equiv \hat{\mathbf{x}}_{\mathbf{N}} - \mathbf{A}_{\mathbf{0}}^{\mathbf{N}}\mathbf{x}_{\mathbf{0}} - \sum_{j=0}^{N-1}\mathbf{A}_{\mathbf{0}}^{\mathbf{j}}\mathbf{B}_{\mathbf{0}}\boldsymbol{\omega}_{\mathbf{p}}\,. \tag{20}$$

The problem is re-formulated in the matrix-vector form such that the adjustment vector, $\boldsymbol{\delta}\mathbf{t}_{\mathbf{N}} \equiv \begin{bmatrix}\delta t_{1N} & \delta t_{2N} & \dots & \delta t_{NN}\end{bmatrix}^{\mathbf{T}}$, is sought such that the target vector is reached:

$$\mathbf{y}_{\mathbf{N}} \Leftarrow \boldsymbol{\Phi}_{\mathbf{N}}\boldsymbol{\delta}\mathbf{t}_{\mathbf{N}} + o(\|\boldsymbol{\delta}\mathbf{t}_{\mathbf{N}}\|_2^2), \tag{21}$$

where

$$\boldsymbol{\Phi}_{\mathbf{N}} \equiv \begin{bmatrix}\varphi_{\mathbf{1N}} & \varphi_{\mathbf{2N}} & \dots & \varphi_{\mathbf{NN}}\end{bmatrix} \tag{22}$$

is the regressor matrix with

$$\varphi_{\mathbf{NN}} \equiv \mathbf{B}_{\mathbf{t}}\boldsymbol{\omega}_{\mathbf{p}}\,, \tag{23}$$

$$\varphi_{\mathbf{mN}} \equiv \mathbf{A}_{\mathbf{0}}\varphi_{\mathbf{m+1,N}}\,,\ m = 1,2,...,N-1. \tag{24}$$

At this point, the assumption that the adjustments are small must be made. It may be justified by the fact the target state and the nominal state both share the same precession angle and the fact that the number of pulse cycles N is typically much larger than the number of elements in the target vector, 4. However, the assumption may still be violated, if the oblateness parameter approaches integer numbers, for which performing precession maneuver and controlling nutation become directly opposing tasks. Parametric study evaluating this assumption is presented in the subsequent sections. Solution to the non-square problem for $N > 4$ using singular value decomposition (SVD) method yields the minimum-norm solution:[7]

$$\boldsymbol{\delta t_N} = {}^{+}\boldsymbol{\Phi_N}\mathbf{y_N}, \tag{25}$$

where

$$\boldsymbol{\Phi_N} = \mathbf{USV^T} \tag{26}$$

is the SVD decomposition of $\boldsymbol{\Phi_N}$ with the pseudo-inverse defined as

$${}^{+}\boldsymbol{\Phi_N} \equiv \mathbf{VS^{-1}U^T}. \tag{27}$$

In the thin SVD formulation, only non-zero singular values are included in the diagonal matrix $\mathbf{S}$.[7]

TREATMENT OF RANK-DEFICIENCY

Inspection of the matrix $\boldsymbol{\Phi_N}$ shows that it may have at most three non-zero singular values. Hence, the problem is underdetermined and rank-deficient at the same time. This means that there exists a subspace in the four-dimensional target vector space, such that the projection of the target vector into that subspace is not affected by the adjustments $\boldsymbol{\delta t_N}$ (under linear assumption). The projection can be computed as follows

$$\tilde{\mathbf{y}}_\mathbf{N} \equiv \left(\mathbf{E} - \mathbf{UU^T}\right)\mathbf{y_N} \neq \mathbf{0}, \tag{28}$$

where $\mathbf{E} \neq \mathbf{UU^T}$ because dimension of $\mathbf{U}$ is $4 \times r$, where the rank $r < 4$. The rank deficiency is generally undesirable as it shows that, if part of the target vector lies in that subspace, it is not reachable by any adjustments. However, with typical $r = 3$, the chances are favorable that the major part of the target vector can be reached. Also, the minimum-norm solution is inherently robust with respect to rank-deficiencies as it simply does not take into account any part of the target vector that lies in that subspace when determining adjustments. In other words, the solution does not try to make adjustments based on the unreachable part of the target vector.

Still, this situation is undesirable and the alternative is to reduce the dimension of the target state (and, hence, the target vector). As it was stated, precession angle targeted by the method is based on the nominal pulsing. It is possible to remove this angle from the state and only seek to have zero nutation and deviation angles. In other words, it is possible to redefine $\boldsymbol{\theta}$ as $\boldsymbol{\theta} \equiv \theta_1$. This essentially means that, instead of letting the unreachable subspace vary from case to case, the subspace is fixed along the precession angle. The idea behind this modification is that zeroing both nutation and deviation angles using small adjustments should put the precession angle near its nominal desired value.

SENSITIVITY ANALYSIS

In practice, none of the assumptions introduced for this method are truly met. Hence, it is important to analyze sensitivity of the results to violations of these assumptions. This section describes analytic techniques for the analysis whereas the next section contains results of the parametric studies.

One of the results can be obtained directly from the method formulation. Sensitivity of the final state to the adjustments and to their additive imperfections is the same provided that the adjustments are small:

$$\frac{\partial \mathbf{x}_\mathbf{N}}{\partial \boldsymbol{\delta}\mathbf{t}_\mathbf{N}} = \boldsymbol{\Phi}_\mathbf{N} \sim (\sigma - 1). \tag{29}$$

The 2-norm of the regressor matrix can also be used as a single measure of that sensitivity:

$$\left\| \frac{\partial \mathbf{x}_\mathbf{N}}{\partial \boldsymbol{\delta}\mathbf{t}_\mathbf{N}} \right\|_2 = \left\| \boldsymbol{\Phi}_\mathbf{N} \right\|_2 = s_1 \sim (\sigma - 1), \tag{30}$$

where s_1 is the largest singular value of $\boldsymbol{\Phi}_\mathbf{N}$.[7] These results indicate that near-symmetrical bodies are less sensitive to pulse adjustments, i.e. they require larger adjustments for the same final state change. The problem completely degenerates for symmetrical bodies ($\sigma = 1$). The results also indicate that small relative timing imperfections cause proportionally small relative state changes. Note that sensitivity of the minimum norm solution to changes in the target vector is proportional to $1/(\sigma - 1)$, which makes this method ill-suited for near-symmetrical bodies. Of course, the concept of precession maneuver itself degenerates for such bodies.

Another result that can be obtained by inspection of the state transition matrices shows that the near-symmetrical bodies are also less sensitive to variations in pulse duration:

$$\frac{\partial \mathbf{x}_\mathbf{N}}{\partial \Delta t} \sim (\sigma - 1) \tag{31}$$

and

$$\left\| \frac{\partial \mathbf{x}_\mathbf{N}}{\partial \Delta t} \right\|_2 \sim (\sigma - 1). \tag{32}$$

Note that, while the transition matrices are generally formulated without small pulse duration assumption, the assumption is practical for efficiency reasons: given the same thrust impulse, shorter pulse is more effective. Hence, simplified transition matrices are also shown in appendix.

Sensitivity to mass property imperfections is also important and has been studied before. It has been shown that closed-form attitude dynamics derived for axisymmetric case remains accurate in the first order of relative inertia errors.[5,6] It has been also shown that the adjustment of precession pulses that targets only nutation cancellation can successfully achieve this even in the presence of significant inertia errors.[6] These results are not extended in this paper, but will be a subject of further review.

PARAMETRIC STUDIES

Parametric studies are presented in this section to supplement the practicality analysis of this method. Measures studied in this section are separated in three categories: linearity measures, accuracy measures and efficiency measures.

Linearity measures serve as indicators for when it is appropriate to utilize proposed time adjustment method. They include maximum magnitude of the adjustment angle, $\max_{k=1,2,\ldots,N}\left|\Omega\delta t_k\right|$, and maximum magnitude of the deviation angle, $\max_{t\in[t_0,t_N]}\left|\theta_1\right|$. The former affects validity of linearization for the minimum-norm solution, the latter affects validity of linearization of Euler angles kinematics. When either one measures exceeds its threshold, the method is no longer valid as it uses inaccurate state transition.

Accuracy measures reflect how close the final state is to the target state. They include the post-maneuver nutation angle, $\Theta_N \equiv \tan^{-1}\dfrac{\left\|\boldsymbol{\omega}_{\mathbf{N}}\right\|_2}{\sigma\Omega}$, and the post-maneuver precession error angle, $\Delta\theta_N \equiv \cos^{-1}\left(\hat{e}_3 \bullet e_3\right)_N$, where $\hat{e}_3, e_3$ represent unit vectors along the desired spin axis and the spin axis achieved after N pulse cycles.

Finally, efficiency measures demonstrate usefulness of the method for saving fuel and time. They include total impulse saved, $I_m \equiv \left\|M\right\|_2\left(\Delta tN + \Delta t_{ANC}\right)$, where Δt_{ANC} is the duration of thrusting during post-maneuver active nutation control (ANC), and maneuver duration reduction, $T_{tot} \equiv TN + T_{ANC}$, where T_{ANC} is the total duration of post-maneuver ANC.

The study is performed using normalized spacecraft model, $I_a = 1$, spinning at the rate $\Omega = 120^\circ/s$ initially at pure spin. The target precession angle is selected as follows: target angle of 20° is used in simplified analysis to determine torque magnitude required to reach it, given the number of pulses and pulse duration. The torque is then applied without time adjustments and the precession angle reached is used as the target. The pulse duration is selected such that it spans 5° of spin angle and the pulse cycle is equal to spin period, $T = 3s$. Performance of the method is illustrated by the time histories of the accuracy measures computed for $\sigma = 1.35$ and $N = 10$, so that maneuver stops after 30 s (Figs.1,2). Dotted line represents nominal performance and solid line represents adjusted performance.

There can be seen a significant reduction in nutation and overall improvement in precession accuracy because of that. These and other measures are evaluated for the following ranges of parameters: the oblateness parameter, σ, from 0.25 to 2 (singularity near 1 is excluded), and the number of pulses, *N*, from 10 to 100.

As expected, the linearity measures improve as more pulses are used (Figs.3,4). They also improve away from integer values of the oblateness parameter. Note that adjustments decrease rapidly near $\sigma = 0.5,1.5$, which is also as expected as those values are known to provide nutation cancellation without adjustments. Similar behavior is exhibited by the accuracy measures (Figs.5-8). Application of the method reduces the post-maneuver nutation dramatically (Figs.5,6), whereas the post-maneuver precession error is typically maintained at least as well (Figs.7,8). The most important results are obtained for the efficiency measures (Figs.9,10). There can be fuel savings of up to 10% for each 20° maneuver (Fig.9). These savings are correlated with the reduction of post maneuver nutation because ANC is comparatively more fuel intensive than pulsing during precession. The maneuver duration reduction is not significant because ANC phase is short compared to precession, which includes relatively long coasting phases. However, note that using more pulse cycles to reach the same precession angle means spending proportionally more time on this maneuver. In other words, if the proposed method does not give much savings for 100 pulse cycle maneuver, but can save 2% of fuel for 50 pulse cycle maneuver, the latter may be employed and duration of the maneuver can be reduced in half.

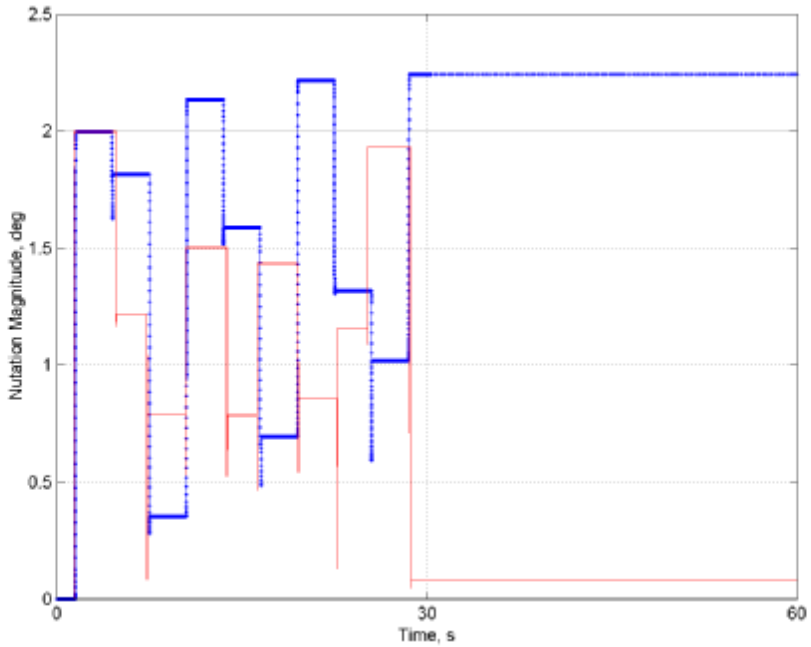

Figure 1 Nutation angle, deg

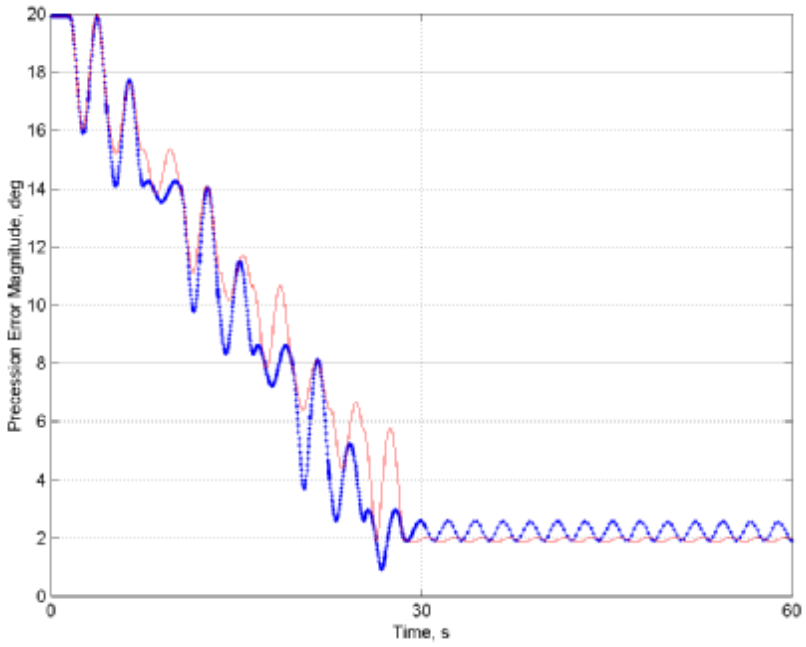

Figure 2 Magnitude of precession error angle, deg

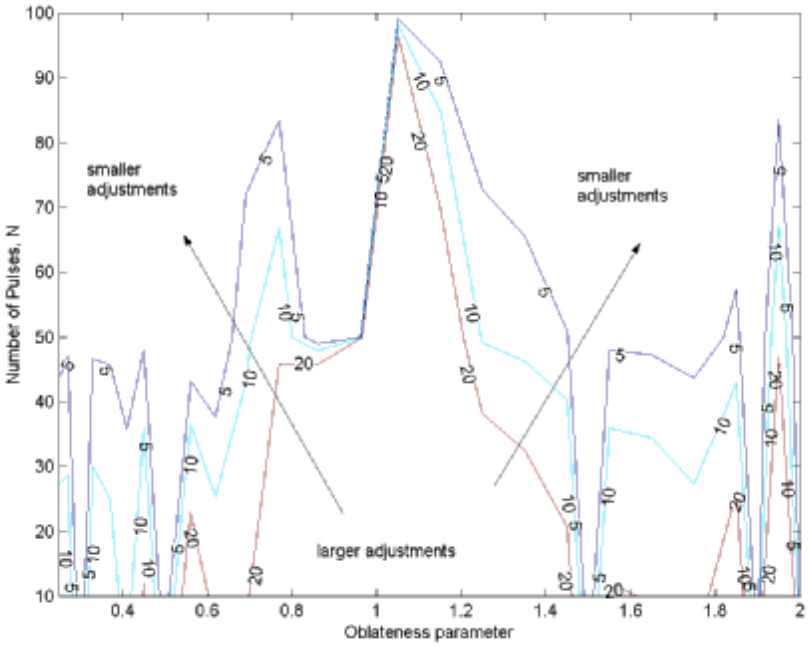

Figure 3 Maximum magnitude of adjustment angle, deg

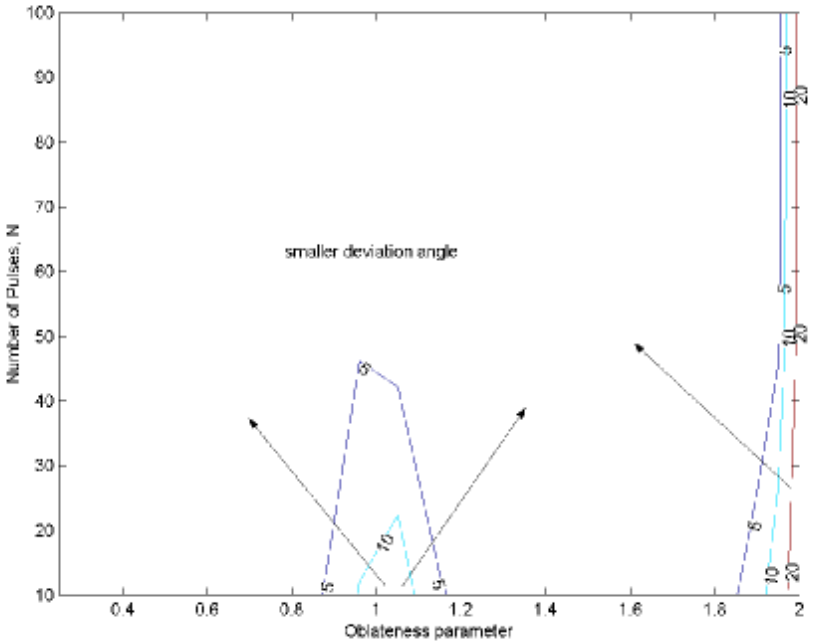

Figure 4 Maximum magnitude of deviation angle, deg

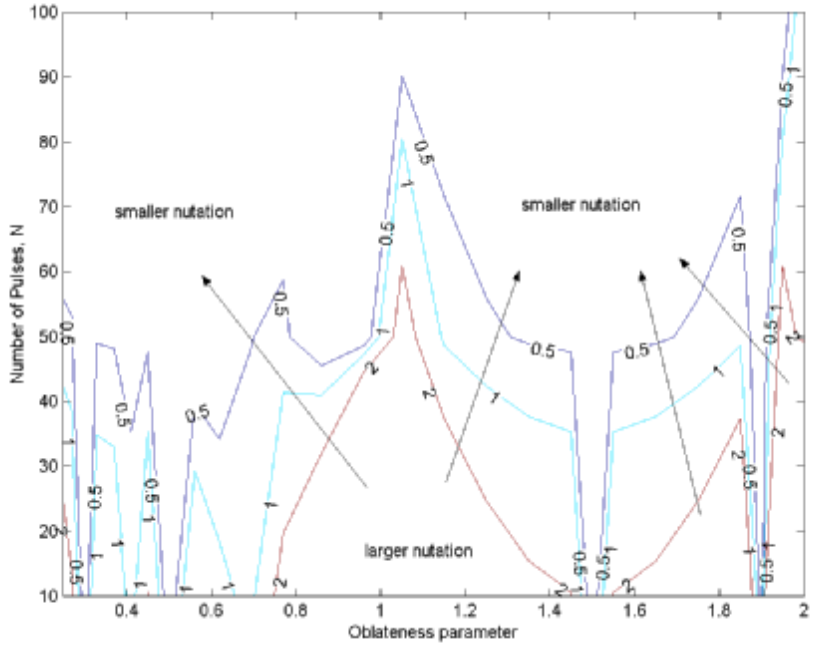

Figure 5 Nominal post-maneuver nutation angle, deg

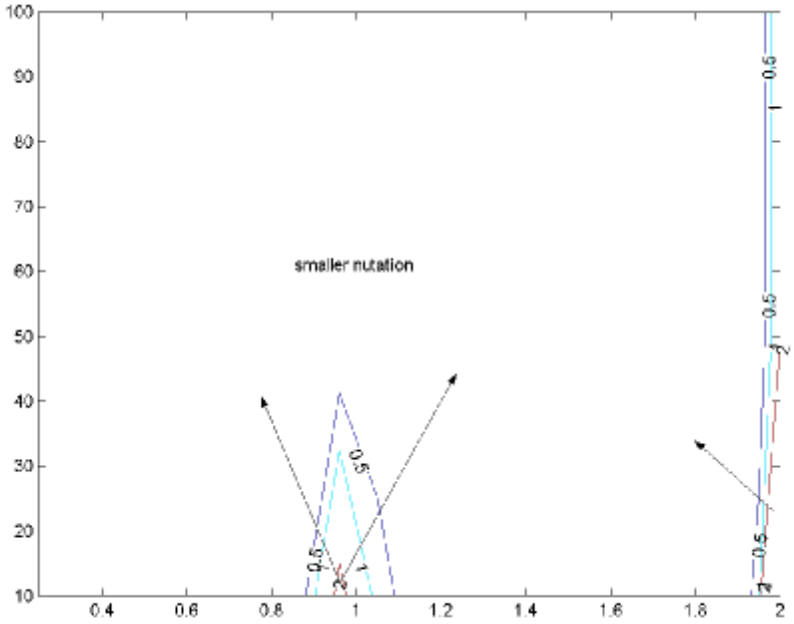

Figure 6 Adjusted post-maneuver nutation angle, deg

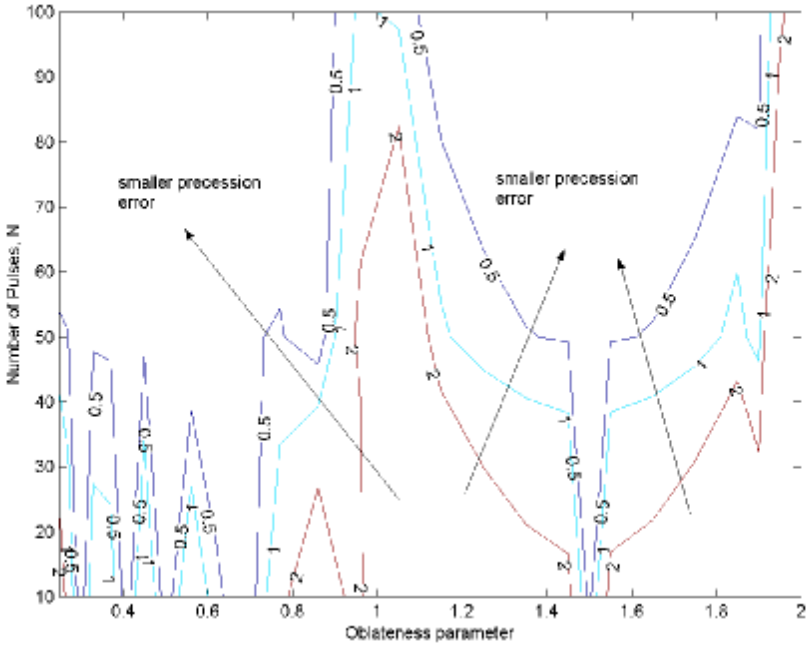

Figure 7 Nominal post-maneuver precession error angle, deg

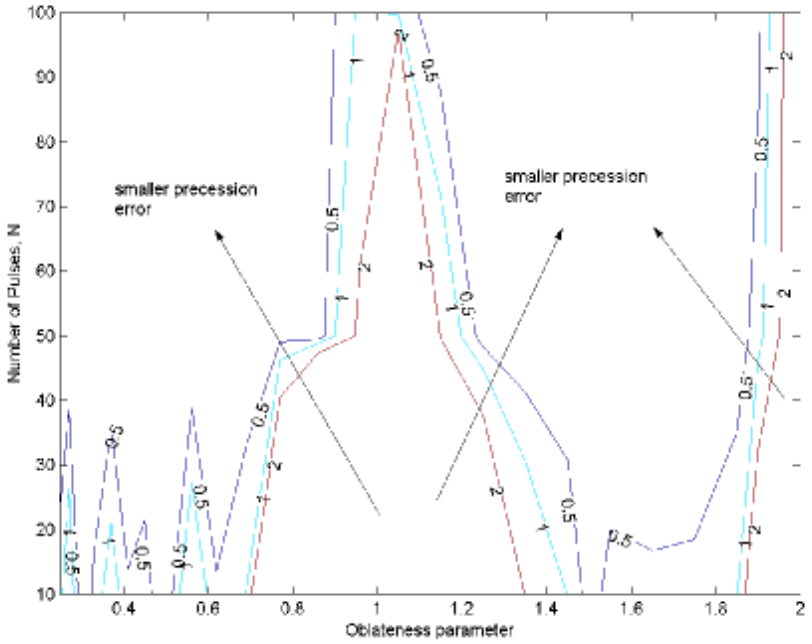

Figure 8 Adjusted post-maneuver precession error angle, deg

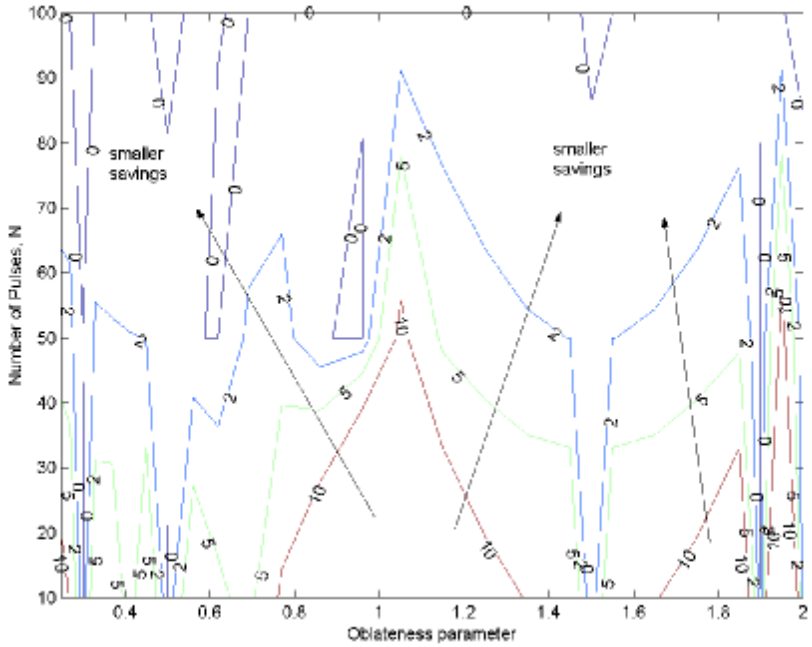

Figure 9 Total impulse saved, %

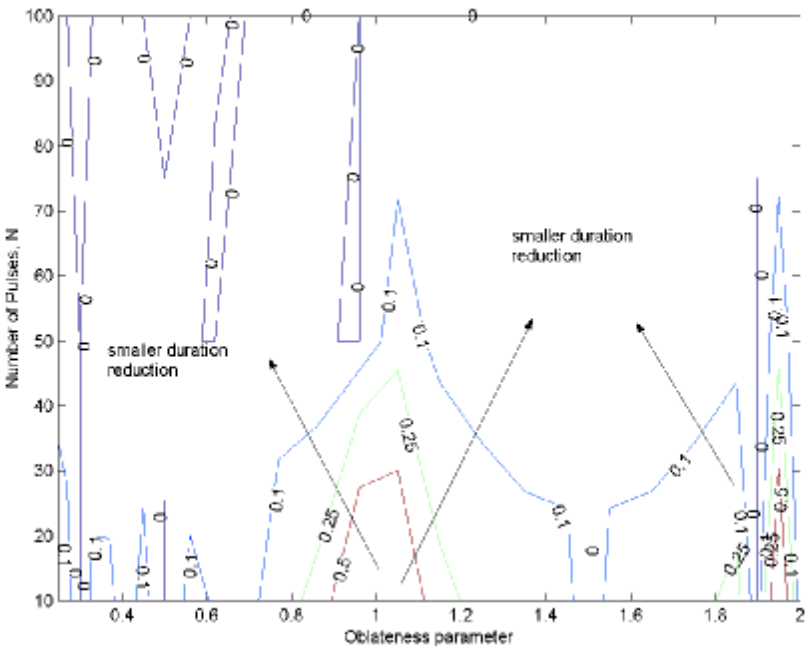

Figure 10 Maneuver duration reduction, %

CONCLUSIONS

The proposed method achieves simultaneous precession maneuver and active nutation control using small adjustments to thruster pulses for a wide range of axisymmetric inertia moments. As a result there can be significant pointing accuracy improvements as well as time and fuel savings.

REFERENCES

1. *Spacecraft Attitude Determination and Control*, J.R. Wertz (ed.), Kluver Academic Publishers, 1978.

2. A.E. Bryson, Jr., *Control of Spacecraft and Aircraft,* Princeton University Press, Princeton, NJ, 1994.

3. M.H. Kaplan, *Modern Spacecraft Dynamics and Control*, Wiley, New York, 1976.

4. B. Wie, *Space Vehicle Dynamics and Control,* AIAA Education Series, AIAA, 1998.

5. S. Tanygin and J. Woodburn, "Sensitivity of Spin-Axis Reorientation Maneuvers," AAS Paper 99-321, AAS/AIAA Astrodynamics Specialist Conference, Girdwood, Alaska, Aug. 16-19, 1999.

6. A.C. Or, "Injection Errors of a Rapidly Spinning Spacecraft with Asymmetries and Imbalances," *the Journal of the Astronautical Sciences*, Vol.40, No.3, 1992, pp.419-427.

7. G.H. Golub and C.F. Van Loan, *Matrix Computations*, 3rd Ed., The John Hopkins University Press, Baltimore, MD, 1996.

APPENDIX

General state transition matrices:

$$\mathbf{A}_{\omega 0} = \mathbf{R}\{2\sigma\pi\}, \tag{33}$$

$$\mathbf{B}_{\omega 0} = \mathbf{R}\left\{\sigma\pi + \frac{(\sigma-1)\Omega\Delta t}{2}\right\} - \mathbf{R}\left\{\sigma\pi - \frac{(\sigma-1)\Omega\Delta t}{2}\right\}, \tag{34}$$

$$\begin{aligned}\mathbf{B}_{\omega t} = {} & (\sigma-1)\Omega\mathbf{R}\left\{\left(\sigma+\frac{1}{2}\right)\pi - \frac{(\sigma-1)\Omega\Delta t}{2}\right\} \\ & -(\sigma-1)\Omega\mathbf{R}\left\{\left(\sigma+\frac{1}{2}\right)\pi + \frac{(\sigma-1)\Omega\Delta t}{2}\right\}\end{aligned}, \tag{35}$$

$$\mathbf{A}_{\theta 0} = \frac{\mathbf{R}\{(2\sigma-1/2)\pi\} - \mathbf{R}\{-\pi/2\}}{\sigma\Omega}, \tag{36}$$

$$\begin{aligned}\mathbf{B}_{\theta 0} = {} & \frac{\mathbf{R}\left\{\left(\sigma+\frac{1}{2}\right)\pi - \frac{(\sigma-1)\Omega\Delta t}{2}\right\} - \mathbf{R}\left\{\left(\sigma+\frac{1}{2}\right)\pi + \frac{(\sigma-1)\Omega\Delta t}{2}\right\}}{\sigma\Omega} \\ & -(\sigma-1)\frac{\mathbf{R}\left\{\frac{\pi-\Omega\Delta t}{2}\right\} - \mathbf{R}\left\{\frac{\pi+\Omega\Delta t}{2}\right\}}{\sigma\Omega}\end{aligned}, \tag{37}$$

$$\mathbf{B}_{\theta t} = (\sigma-1)\frac{\mathbf{R}\left\{\frac{-\Omega\Delta t}{2}\right\} - \mathbf{R}\left\{\frac{\Omega\Delta t}{2}\right\}}{\sigma} + (\sigma-1)\frac{\mathbf{R}\left\{\sigma\pi - \frac{(\sigma-1)\Omega\Delta t}{2}\right\} - \mathbf{R}\left\{\sigma\pi + \frac{(\sigma-1)\Omega\Delta t}{2}\right\}}{\sigma}. \quad (38)$$

State transition matrices simplified under the small pulse duration assumption: $|\Omega\Delta t| << 1$:

$$\mathbf{B}_{\omega 0} \approx (\sigma-1)\Omega\Delta t\mathbf{R}\left\{\left(\sigma+\frac{1}{2}\right)\pi\right\}, \quad (39)$$

$$\mathbf{B}_{\omega t} \approx (\sigma-1)^2\Omega^2\Delta t\mathbf{R}\{\sigma\pi\}, \quad (40)$$

$$\mathbf{B}_{\theta 0} \approx (\sigma-1)\Delta t\frac{\mathbf{R}\{\sigma\pi\}+\mathbf{E}}{\sigma}, \quad (41)$$

$$\mathbf{B}_{\theta t} \approx \frac{(\sigma-1)^2\Omega\Delta t}{\sigma}\mathbf{R}\left\{\left(\sigma-\frac{1}{2}\right)\pi\right\} - \frac{(\sigma-1)\Omega\Delta t}{\sigma}\mathbf{R}\left\{\frac{\pi}{2}\right\}. \quad (42)$$